Boletín Geológico

SERVICIO GEOLÓGICO COLOMBIANO

Boletín Geológico, 48(Spl.1), 11-24, 2021

https://doi.org/10.32685/0120-1425/bol.geol.48.Spl.1.2021.586

Received: June 22, 2021

Revision received: September 1, 2021

Accepted: September 9, 2021

Published online: October 5, 2021

Case study article

Regional integration and 3D modeling of airborne geophysical data: Map of Geophysical Anomalies of Colombia for mineral resources, 2020 version

Integración regional y modelado 3D de datos geofísicos aerotransportados: Mapa de anomalías geofísicas de Colombia para recursos minerales, versión 2020

Manuel **Puentes**[1], Adriana **Robayo**[1], Ismael **Moyano**[1], Eduardo **Henrique**[2], Marcela **Lara**[1], Hernán **Arias**[1], Diana **Ospina**[1], Óscar **Rojas**[1], Ernesto **Gómez**[1], Sergio **Torrado**[1], Gloria **Prieto Rincón**[1]

1. Servicio Geológico Colombiano, Dirección de Recursos Minerales, Grupo de Investigación en Geoquímica y Geofísica Aplicada, Bogotá, Colombia
2. Consultant, São Paulo, Brasil
Corresponding author: Manuel Puentes, mpuentes@sgc.gov.co

Abstract

The *Map of Geophysical Anomalies of Colombia for mineral resources, MAGC 2020 version* compiles the geophysical information acquired, processed and interpreted by the Servicio Geológico Colombiano (SGC) since 2013. This information was collected via airborne platforms (aircrafts) using magnetometry and gamma spectrometry. This version covers approximately 547 960 km^2 of the national territory in the Andean (North and Central), Eastern (Eastern Plains and Amazon) and Caribbean zones (Perijá mountain range). This information consists of 17 blocks of geoscientific interest, covered by flight lines separated by 500 and 1000 m, for a total of more than 907 566 linear km of airborne information, acquired at a nominal altitude of 100 m above the ground, with a sampling resolution that was not previously available at this scale and coverage. This document presents the methodology for compiling, processing and representing the thematic coverage included in MAGC 2020: Map of *Total field magnetic anomaly* (TFMA), *Map of the analytic signal (AS)* and *radiometric ternary map of the distribution of the relative concentrations of uranium, thorium and potassium*. Furthermore, the work identifies 1079 magnetometric anomalies of interest, which were subsequently analyzed and modeled in the *Map of magnetic sources modeled from magnetization vector inversion*, which contains a total of 1297 magnetic bodies interpreted from these anomalies. Integration of available geological and metallogenic information with each of these bodies allow the suggestion of possible geological sources and possible exploration targets. The objectives of this study were

Citation: Puentes, M., Robayo, A., Moyano, I., Henrique, E., Lara, M., Arias, H., Ospina, D., Rojas, O., Gómez, E., Torrado, S., & Prieto, G. (2021). Regional integration and 3D modeling of airborne geophysical data: Map of Geophysical Anomalies of Colombia for mineral resources, 2020 version. *Boletín Geológico, 48* (Spl.1), 11-24. https://doi.org/10.32685/0120-1425/bol.geol.48.Spl.1.2021.586

to generate and integrate geophysical information to identify new areas of interest with regards to potential mineral resources, and to generate new geoscientific knowledge about Colombia for land-use planning.

Keywords: Magnetic anomaly, magnetometry, gamma spectrometry, total-field magnetic anomaly (TFMA), analytic signal (AS), 3D inversion, 3D modeling.

RESUMEN

El *Mapa de anomalías geofísicas de Colombia* para recursos minerales, versión 2020 (MAGC 2020), compila la información geofísica adquirida, procesada e interpretada por el Servicio Geológico Colombiano (SGC) desde el año 2013. Esta información se ha levantado mediante plataformas aerotransportadas (aviones), utilizando magnetometría y gamma espectrometría y, para esta versión, abarca cerca de 547 960 km^2 del territorio nacional, distribuidos en la zona andina (norte y centro), zona oriental (Llanos orientales y Amazonía) y zona caribe (Serranía del Perijá). Esta información representa 17 bloques de interés geocientífico, que fueron cubiertos con líneas de vuelo separadas entre 500 y 1000 m, para un total de más de 907 566 km lineales de información aerotransportada, adquirida a una altura nominal de 100 m sobre el terreno y con una resolución de muestreo que hasta la fecha no estaba disponible a esta escala y cubrimiento. Este documento presenta la metodología de compilación, procesamiento y representación final de las coberturas temáticas incluidas en el MAGC2020: *Mapa de anomalía magnética de campo total* (ACT), *Mapa de señal analítica* (SA) de la ACT y *Mapa radiométrico de distribución ternaria de la concentración relativa de uranio, torio y potasio*. Además, la identificación de 1079 anomalías magnetométricas de interés, cuyo posterior análisis y modelamiento 3D están representados en el Mapa de fuentes magnéticas modeladas a partir de la inversión del vector de magnetización, que contiene un total de 1297 cuerpos magnéticos interpretados a partir de estas anomalías. El objetivo de este trabajo es generar e integrar información geofísica para identificar nuevas áreas de interés con potencial en recursos minerales y generar nuevo conocimiento geocientífico de Colombia que sirva como herramienta para la toma de decisiones en planeación y del ordenamiento territorial colombiano.

Palabras clave: Anomalía magnética, magnetometría, espectrometría gamma, anomalía magnética de campo total (TFMA), señal analítica (AS), inversión 3D, modelado 3D.

1. Introduction

Since 2012, the Servicio Geológico Colombiano (SGC) has been advancing the acquisition of geophysical information using magnetometry and gamma spectrometry, with a regional coverage and spatial resolution that were previously not available for Colombia (Moyano et al., 2016). Although prior to this geophysical survey, government entities such as Ecopetrol and the Agencia Nacional de Hidrocarburos (ANH) had conducted airborne geophysical studies, the regional nature and technical parameters of these surveys (altitude, sampling density and resolution) were not detailed enough to detect magnetic anomalies originating from relatively small geological bodies, because as the altitude increases, the magnetic intensity of the latter decreases and is masked by larger regional anomalies. In contrast, the information acquired by the SGC and represented in the *Map of Geophysical Anomalies of Colombia for mineral resources – MAGC 2020 (*Moyano et al., 2020*)* reflects acquisition parameters at a much more detailed scale, allowing us to identify and characterize new deposits of minerals and to complement geological mapping.

The survey of airborne geophysical information is based on the need to expand the geoscientific knowledge of the national territory, generate useful information to identify potential mineral resources, provide basic information for better land-use planning, generate geological cartography and advance geoscientific research. Anomalies in the magnetic field are related to variations in the physical properties (magnetic susceptibility) of the materials which compose the earth's crust, which in turn directly reflect the concentration of magnetic minerals in the rocks that constitute them. From a geological-geophysical perspective, magnetic anomalies can be related to a wide variety of geological sources, such as intrusive bodies, dikes, hydrothermal alteration zones and volcanism.

All the geophysical airborne information collected since the first SGC survey in 2012 was processed and integrated, and then presented as four layers of information, including: 1) the total field magnetic anomaly map, 2) the analytical signal map

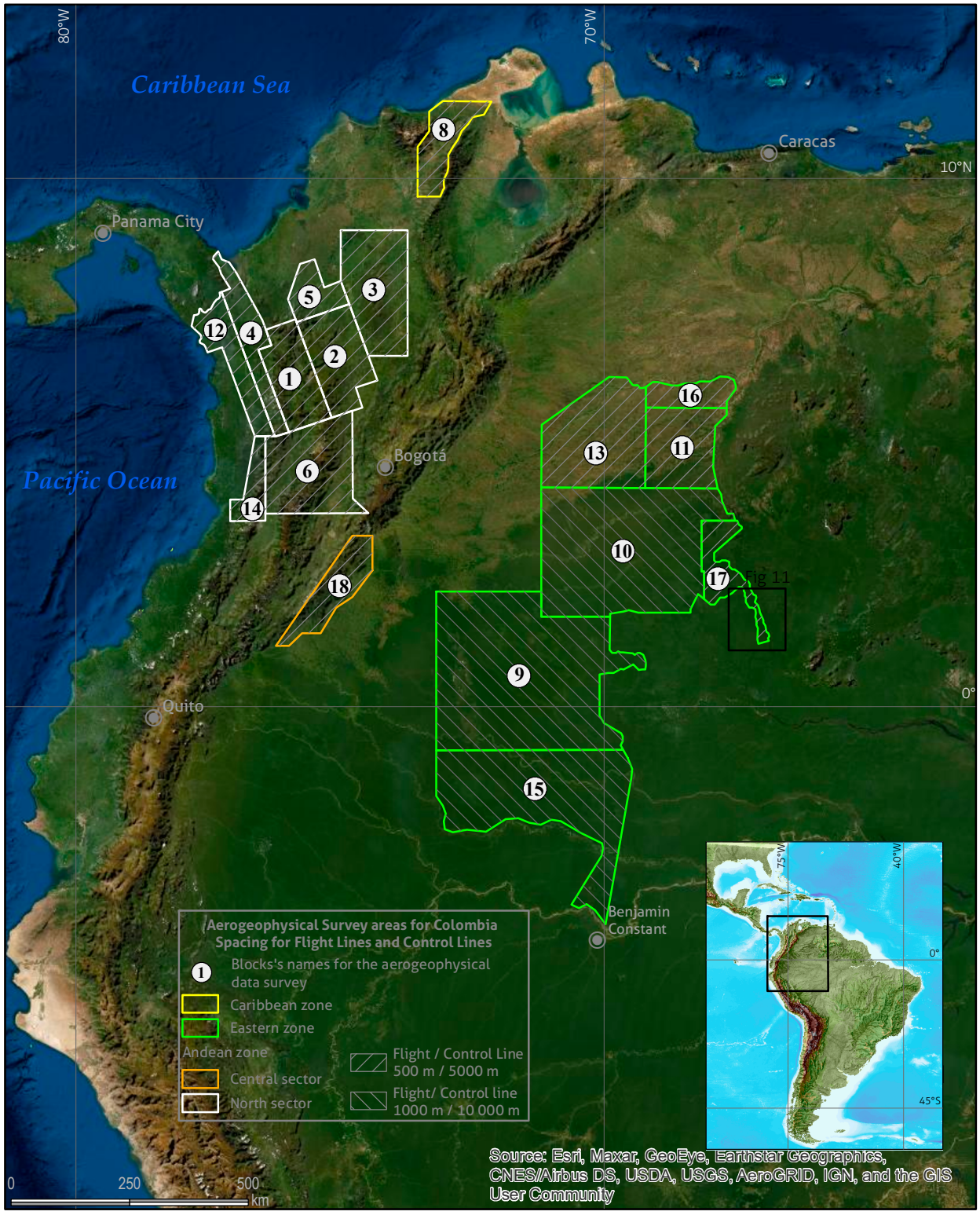

Figure 1. Location of the 17 blocks containing the airborne geophysical information
The color of each block corresponds to the geographical region (green: Amazonas-Orinoquía; blue: North Andean; Orange: Central Andean; Yellow: Caribbean) and the hatching indicates the distance between flight lines (NE-SW: 500 m, NW-SE: 1000 m).

of the total field magnetic anomaly, 3) the ternary radiometric map of the concentration distribution of uranium, thorium and potassium and 4) the map of possible geological sources, based on modeled magnetic sources, 2018 version (Moyano et al., 2018), which includes magnetic sources from the Córdoba and Garzón blocks for the 2020 version. The possible geological sources were identified and interpreted according to their geophysical attributes during modeling and characterized as being in a geological and/or metallogenic environment, information available from the *Metallogenic Map of Colombia 2020* (Sepúlveda et al., 2020) together with the *Geological Map of Colombia 2015* (Gómez et al., 2015).

The four layers generated allowed us to produce the 2020 version of the MAGC (Moyano et al., 2020), featuring magnetometry and gamma ray spectrometry information collected for 17 blocks (Figure 1). This map shows magnetic and gamma ray spectrometric anomalies. One of the blocks (Cesar-Perijá) is located in the Caribbean area, in the departments of Cesar and La Guajira, in the area of influence of the Sierra Nevada de Santa Marta, with heights ranging between 0 and 3000 meters above sea level. Eight blocks (Antioquia-W, Antioquia-E, Bolívar, Urabá, Andes-N, Darién, Córdoba and Buenaventura) are located in the northern part of the Andean zone. One block (Garzón) is located in the central part of the Andean Zone. In general, the Andean region is located in the departments of Antioquia, Bolívar, Boyacá, Caldas, Cesar, Córdoba, Cundinamarca, Chocó, Huila, Risaralda, Santander, Sucre, Tolima and Valle del Cauca, in Central and Western mountain ranges confluence area, with altitudes ranging from 0 to 5200 m. The seven remaining blocks (Amazonas-N, Guainía, Vichada, Vichada-W, Amazonas-S, Vichada-N and Guainía-E) are located in eastern Colombia, in the departments of Amazonas, Arauca, Caquetá, Casanare, Guainía, Guaviare, Meta, Vaupés and Vichada, areas of gentle slopes and heights that range between 50 and 800 meters above sea level.

1.1. Survey Specifications

All the blocks were surveyed via airborne platforms fixed wing aircrafts that flew at a nominal altitude of 100 m above the ground, where topographic (particularly in the Andean zone) and operational safety conditions allowed. Each aircraft was equipped with a high-precision positioning system and magnetic and gamma spectrometry sensors configured to record variations in the earth's magnetic field, and count radiogenic particles at rates of 10 Hz and 1 Hz respectively. The magnitude of the total magnetic field was measured every 7m to 9m, and the intensity of the natural gamma radiation from the ground was measured every 70 to 90 m. The distance between flight lines for 14 of the 17 blocks was 500 m. The remaining three blocks, located in the Colombian Amazon, were overflown with a distance between flight lines of 1000 m, and crossed by perpendicular control lines separated by 5000 or 10 000 m. The direction of the flight lines was N20W in the Córdoba, Darién, Urabá, Antioquia W and Antioquia E blocks, and N-S in the other blocks. To level the magnetic data, control lines perpendicular to the flight lines were established at distances of 5000 (blocks with flight lines every 500 m) or 10 000 m (blocks with flight lines every 1000 m).

The magnetometry data were acquired using cesium vapor magnetometers in the aircraft in a *tail stinger* installation. This type of assembly requires compensating for the aircraft movements during flights. The following are the technical specifications for the magnetometers installed in the aircraft:

- Sensitivity 0.01 nT
- Absolute accuracy ± 10 nT
- Dynamic range 20 000 and 100 000 nT
- Sampling interval 0.1 seconds (10 Hz)
- Heading effect < 2 nT

Diurnal variations in the magnetic field were recorded by a ground base station, with a sampling interval of no more than 3 seconds, synchronized with the magnetometer in the aircraft. The diurnal variations had a maximum tolerance of 3 nT (peak to peak) for a period of one minute for the magnetic base station. Fluctuations above these values and persisting for more than one hour are considered a possible solar storm, meaning flights were cancelled.

Likewise, 2048 cubic inch NaI Tl (sodium iodide crystals treated with thallium) gamma ray spectrometers were used onboard the aircraft to record the full spectrum of gamma rays between 512 and 1024 channels, at a sampling rate of one per second (1Hz). In addition, upward-looking NaI scintillator detectors were used to record the concentration of atmospheric radon. The K, U and Th counts were extracted from the full spectrum during processing according to their energy levels.

In some areas with special topographic or safety characteristics, the aircraft had to be flown at higher altitudes than the nominal flight value. This higher altitude resulted in progressive deterioration and a loss of sensitivity of the gamma spectrometry equipment, which is reflected as noise in the generated data

and can lead to erroneous interpretations. For this reason, an analysis of the relative concentrations of the uranium (U), thorium (Th) and potassium (K) channels was performed directly from each block's database. From this analysis, data acquired at an unusual height above the nominal 100 meters showed discordant or even negative values of one or all the radioelements, and can be recognized as along-flight line strips of very high or low counts. These noise measurements were represented independently on the ternary gamma spectrometry map, with a warning regarding the interpretation of these areas.

The airborne magnetometry and gamma ray spectrometry information was compiled, integrated, and processed to generate thematic layers (images) with a spatial resolution of 125 m in the Caribbean and Andean zones and 250 m in the Eastern zone (Amazonas and Orinoquía).

2. Method

This section describes the methodology and processing to generate the thematic layers for the Caribbean, Andean (North and Central) and Eastern zones. Interpolation methods and micro leveling (MIC) techniques were applied to the 17 selected blocks, which were grouped along the Caribbean, Andean (North and Central) and Eastern zones. From this processing, three thematic images were generated: *total-field magnetic anomalies* (TFMA), *analytic signal* (AS) and the Ternary map of the distribution of potassium (K), thorium (Th) and uranium (U) concentrations. Subsequently, the magnetic anomalies were identified using magnetometry data. Therefore, to determine spatial characteristics and magnetic susceptibility, the magnetization Vector Inversion (MVI) algorithm was used to process magnetic field data acquired. From the intensity of the magnetic field data (TFMA) of detected anomalies, the MVI generates a mathematical modeling of a volume of data that represents the variations and the values of magnetic susceptibility in the field. Ideally, the inversion of the magnetic anomaly generated by this magnetic susceptibility model is matched to the geometry by the observed TFMA values, and the analytical signal. Finally, a layer was produced with the selected and modeled anomalies.

2.1. Interpolation method for thematic layers

For the interpolation of the magnetometry and gamma ray spectrometry data, a cell size between ¼ and ⅛ was chosen for the spacing of the flight lines, to avoid information loss and recover all frequencies. An appropriate algorithm that maintains the values of the original points while generating a continuous and smoothed surface must be chosen. The most commonly used interpolation algorithms are bidirectional, minimum curvature, weighted inverse distance and kriging methods (Watson and Philip, 1985; Briggs, 1974) algorithms.

For the interpolation of the magnetometry data, the bidirectional algorithm was used. This method correlates data taken line by line, by applying cubic splines both along and through the flight lines following a defined grid interval. Additionally, a low-pass filter is applied to remove high frequencies that generate artifacts in the information. This interpolation method is suitable for this type of survey, in which the data are distributed in parallel lines, because it interpolates first in one direction and then in the orthogonal directions, thus fitting an unlimited number of data points. This algorithm cannot be used for data with a random distribution.

The weighted inverse distance method was applied to the gamma spectrometry data. The sampling points values were calculated using their weighted average in a defined search radius. The weight assigned to each value is inversely proportional to its distance. The weighting of each value is assigned by a power parameter that modulates the influence of each data value as a function of distance. The higher the power parameter is, the more influence it will have on the closest points. In addition, the method adds a weighted slope factor that moderates the sharpness of the values' weights, preventing said values from leaving their range in the vicinity of their points.

2.2. Micro leveling of the thematic layers

Micro leveling is the elimination of residual errors produced in the regular course of a process such as leveling. These errors are manifested as corrugations along lines that are false artefacts (i.e., non-geological effects), creating distorted images identified as noise, while some data points appear in the same direction as the flight lines. This type of noise was removed from the interpolated grids using directional filters applied to the flight and control lines. The micro-leveling technique developed by Minty (1991) removes the non-geological effects caused by residual and leveling errors without affecting the data frequency spectrum.

2.3. Processing of magnetic images

To process and generate the magnetometric layers, it was necessary to apply frequency range filters in the areas, to com-

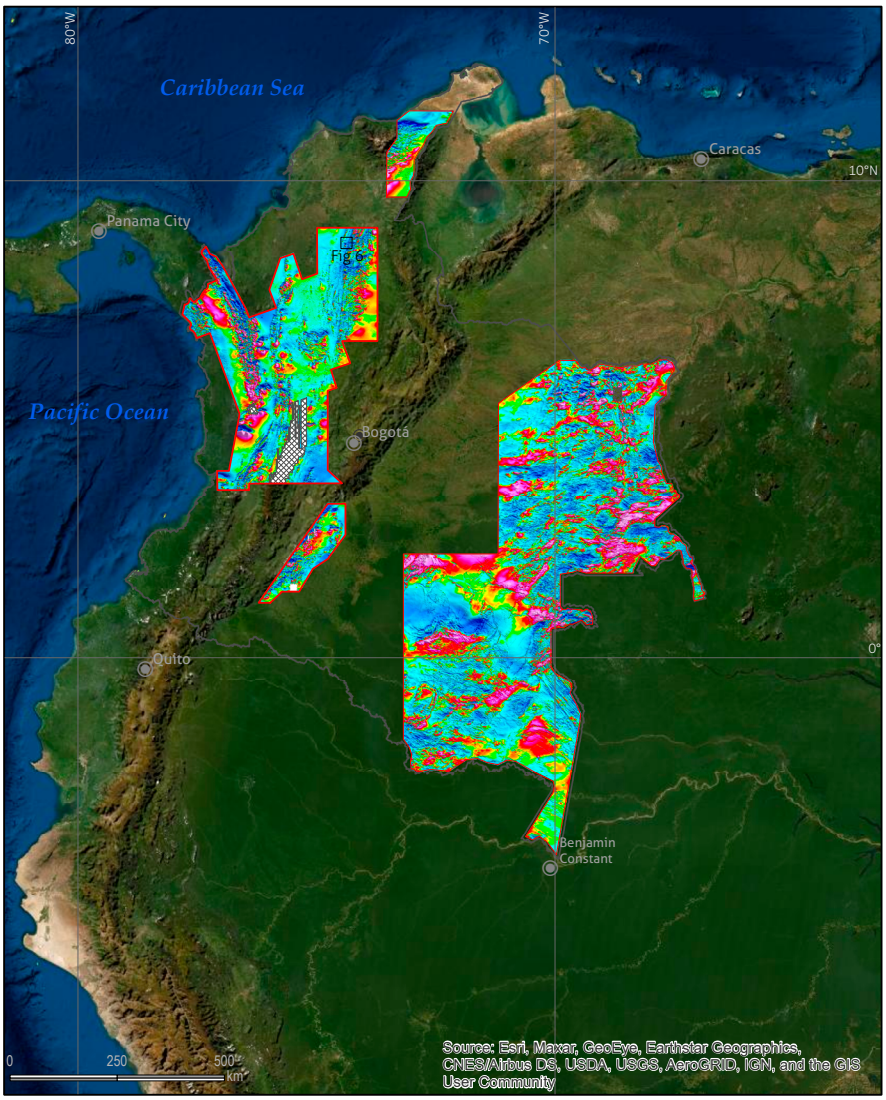

Figure 2. Geophysical anomalies map of Colombia for mineral resources: total-field magnetic anomaly (TFMA)
▨: area not covered.

pensate for noise effects in the leveling and in the combination of some images. The Andean zone (north sector) is the result of combining the images of Antioquia-W, Antioquia-E, Bolívar, Urabá, Andes-N, Darién, Buenaventura and Córdoba. Its processing was more exhaustive, as its leveling was more complex due to the steep topography of the area. For processing, directional and frequency range filters were applied to compensate for the combining of the images. For the Eastern zone, which is composed of the Amazonas-N, Guainía, Vichada, Vichada-W, Amazonas-S, Vichada-N and Guainía-E blocks, the images were combined to generate the TFMA image in this area.

2.3.1. Total-field magnetic anomaly map

The TFMA map (Figure 2) is obtained by removal of temporal variations and geomagnetic field model data (International Geomagnetic Reference Field (IGRF)) (Thébault et al., 2015) from the observed magnetic field. Thus, the TFMA map shows variations in the magnetic field produced by the presence of magnetic sources in the subsurface. However, to generate this image, each zone was processed differently according to the topographic characteristics and the location of the blocks.

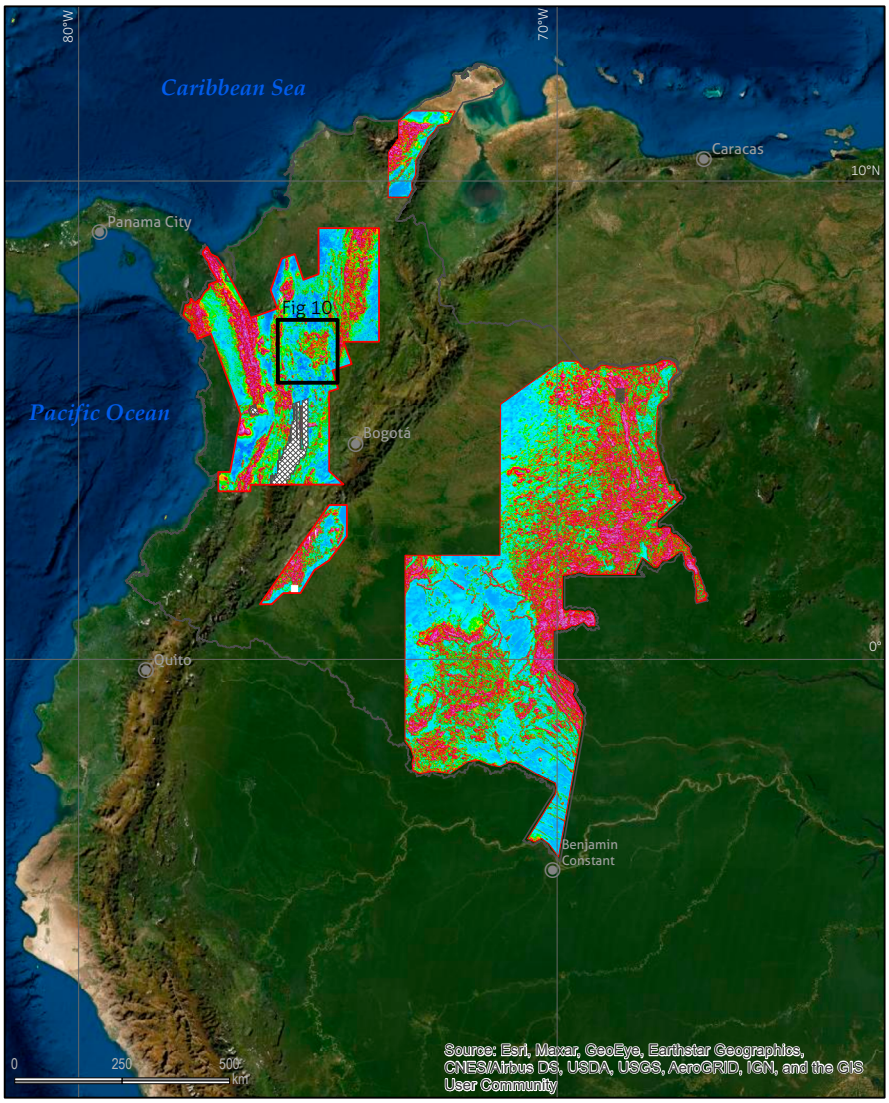

Figure 3. Map of geophysical anomalies of Colombia for mineral resources: analytic signal of the TFMA
▨: area not covered.

2.3.2. TFMA analytic signal

The TFMA analytic signal map (Figure 3) was obtained by applying a mathematical algorithm to the total magnetic field. The variations in the three spatial components in relation to depth were calculated (Roest et al., 1992). This mathematical process was used to highlight the edges of the magnetic sources and to directly locate magnetic anomalies, as this filter is independent of the direction of magnetization.

2.4. Preparation of thematic layers for gamma spectrometry data

To generate this coverage, the weighted inverse distance interpolation method was used for each block's gamma spectrometry data. The images were generated with a spacing of 125 m in the Caribbean and Andean zones (North and Central) and 250 m in the Eastern zone. All the images had a power parameter of 2 and a weighting slope of 1. The gamma spectrometry distribution ternary map shows the composition, in RGB colors, of the relative concentration of the three radioelements potassium (red), thorium (green) and uranium (blue). This composite image was generated from the normalization of the counts

of each of these three elements in the gamma ray spectrometry data, generating the modulation of the red, green and blue colors in proportion to the concentration of potassium, uranium and thorium. The ternary image reduces the effects of gamma ray attenuation by vegetation or soil moisture (International Atomic Energy Agency, 2003). These colors are quantitatively related in a color triangle that indicates the composition of each radioelement channel to which it belongs (see Figure 4).

The processing of the images generated in the Caribbean, Andean (North and Central) and Eastern zones used a multiplication factor to level some images and join them. This factor was applied as the aircraft measurement systems for each block had a different calibration, yielding differing gamma ray counts. In some areas, aircraft were unable to maintain the nominal altitude due to abrupt topography, which reduced the

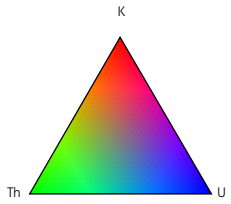

Figure 4. RGB composition of gamma spectrometry data
Red: potassium indicator; green: thorium indicator; blue: uranium indicator. Modified from International Atomic Energy Agency (2003).

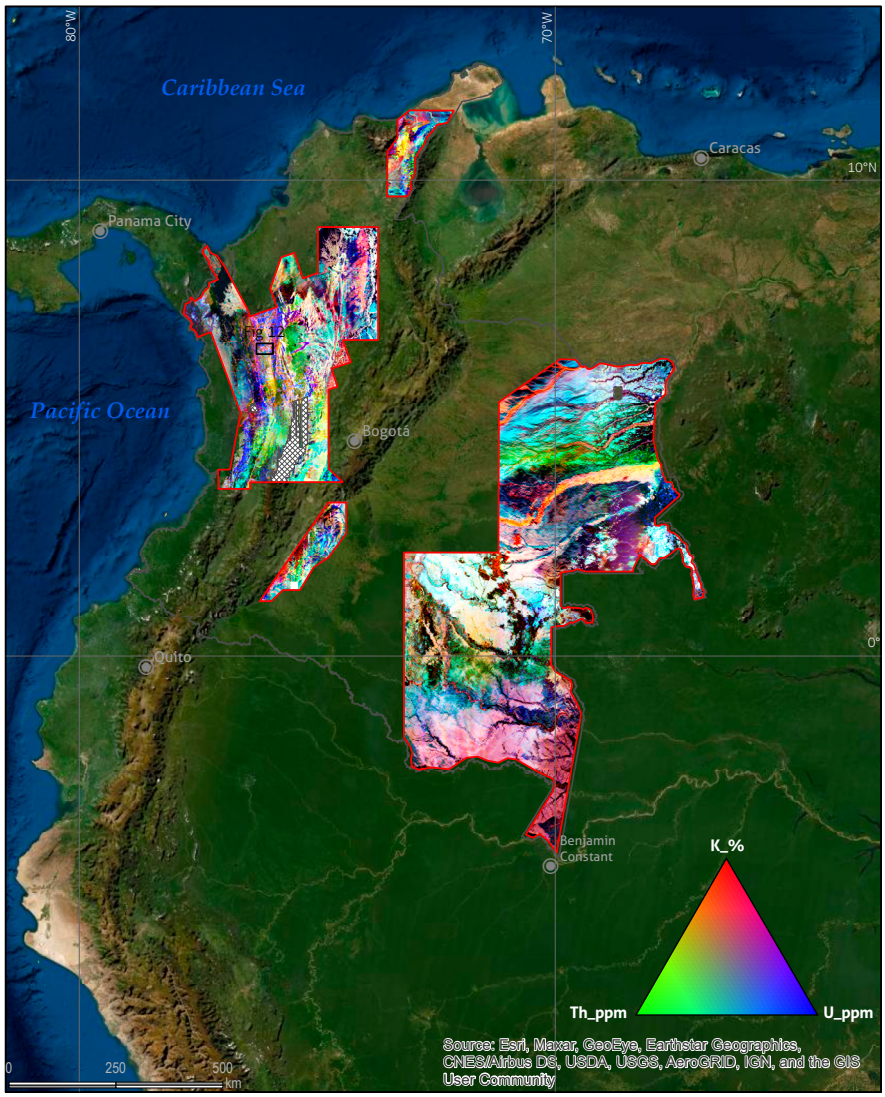

Figure 5. Geophysical anomalies map of Colombia for mineral resources
Ternary map showing the distribution of the potassium (K), thorium (Th) and uranium (U) concentrations.
▨: area not covered.

counts of radioelements potassium (K), thorium (Th), and uranium (U) on the ground. This problem was corrected using deconvolution and height correction techniques to avoid topography effects (Gunn and Almond, 1997). Figure 5 presents the *Ternary map of the distribution of K, Th and U concentrations compiled for Colombia*.

2.5. Selection of magnetic anomalies, 3D modeling and integration of magnetic sources

One of the main objectives of magnetometry information analysis is the identification of areas displaying characteristics associated with the presence of more magnetic bodies than the background. These magnetic anomalies are identified by characteristic attributes in the magnetic information, such as the presence of dipoles in the TFMA map (Figure 6a), areas with magnetic highs in the reduction to pole (RTP) of the TFMA (Baranov, 1957) (Figure 6b) and strong amplitudes of the TFMA analytic signal (Nabighian, 1972) (Figure 6c).

Magnetic anomalies are related to a wide variety of geological sources. Therefore, their geometric and physical parameters must be determined. For this, the magnetization Vector Inversion (MVI) algorithm was used to process acquired magnetic field data affected by remanent magnetization as well as induced magnetization. Remanent magnetization changes the intensity and direction of the total magnetization vector, and thus the magnetic susceptibility. Therefore, remanent magnetization can distort the inversion, if it is assumed that the source is only generated by induced magnetization (Ellis et al., 2012). From the intensity of the magnetic field data (TFMA) for detected anomaly, the MVI generates a mathematical modeling of a volume of data that represents the variations and the values of magnetic susceptibility in the field. Ideally, the inversion of the magnetic anomaly generated by this magnetic susceptibility model is matched to the geometry as observed with TFMA values and the analytical signal.

Finally, the integration of the information on magnetic sources in the blocks of interest was carried out to identify and interpret a possible geological source and exploratory target. For this reason, modeled magnetic sources for each of the 17 blocks were designated following a code consisting of four uppercase alphabetic characters. To identify the geophysical anomalies, a consecutive 3-digit numeric code was used, whilst an alphabetic code (consisting of capital letters, from the letter A to the letter Z) was used for anomalies that required subdividing due to having more than one body. This code is reset for each work block (Table 1). For example: BOLI002, ANTW002A or ANDN002B.

Table 1. Coding of the blocks produced by the airborne geophysical survey

N.° block	Block	Code
1	Antioquia-W	ANTW
2	Antioquia-E	ANTE
3	Bolivar	BOLI
4	Urabá	URAB
6	Andes-N	ANDN
8	Cesar-Perijá	CSPR
9	Amazonas-N	AMZN
10	Guainía	GUAI
11	Vichada	VICH
12	Darien	DARI
13	Vichada-W	VICW
14	Buenaventura	BVNT
15	Amazonas-S	AMZS
16	Vichada-N	VICN
17	Guainía-E	GUAE
18	Garzón	GARZ
19	Córdoba	CORD

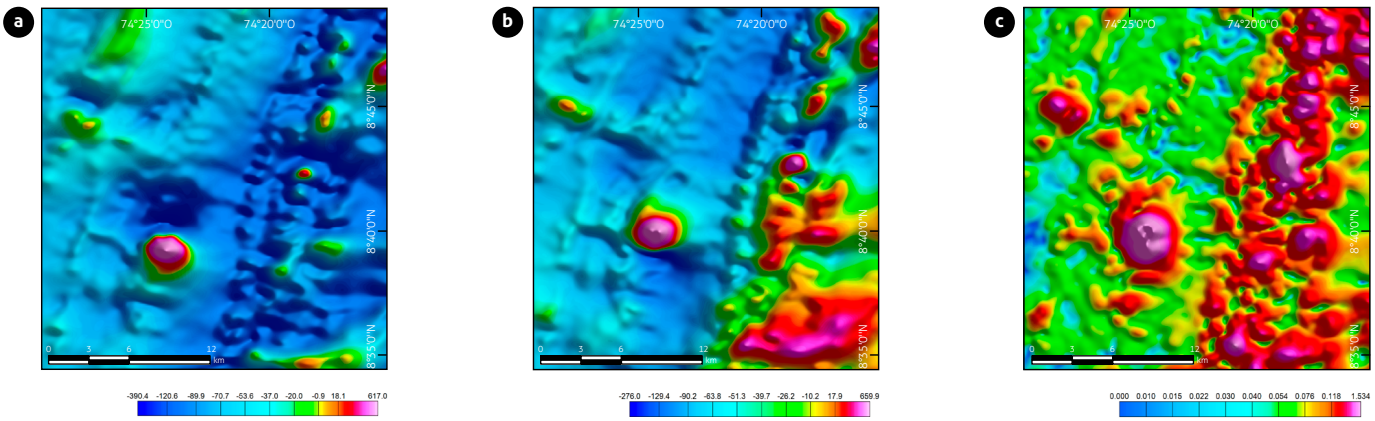

Figure 6. Magnetic source: BOLI022, characterization of the magnetic coverage attributes
a) TFMA; b) RTP; c) AS. See general location in Figure 2

3. Results

3.1. Interpretation of possible geological sources and exploration targets

The resulting compilation of the modeled magnetic sources for each of the 17 blocks is presented in the *Map of magnetic sources modelled by magnetization vector inversion (MVI)* (Moyano et al., 2020). The map presents the magnetic sources identified, characterized by their geophysical attributes during modeling and their geological and/or metallogenic environment (Figure 7). Accordingly, the integration of the magnetic sources for the MAGC 2020 was carried out taking into account the geophysical and geological attributes of the deposits, as per the Metallogenic context provided by the Metallogenic Map of Colombia (MMC), version 2020 (Sepúlveda et al., 2020). Within this context, each anomaly may be correlated with either some identifiable surface geological feature, or with a deep geological source devoid of surface expression (intrusive bodies, dikes, hydrothermal alteration zones, volcanism, faults, among others).

In accordance with the above, the interpretation of a possible geological source for each identified magnetic source refers to the available geological cartography, as per the Geological Map of Colombia (Gómez et al., 2015) for the evaluated area, from which the lithological correlation of the evaluated anomaly is established. As an example of the above, Figure 8 shows the 3D inversion model of the ANTW37B magnetic source, a shallow source associated on the surface with porphyritic basalt, and andesites. Similarly, although the magnetic sources do not have a surface geological expression, the existence of common characteristics to a source with geological correlation allows us to infer a possible similar geological origin. As an example of the above, Figure 9 shows the response in the ACT map and the 3D susceptibility model of the ANTW041 deep magnetic source defined as intrusive.

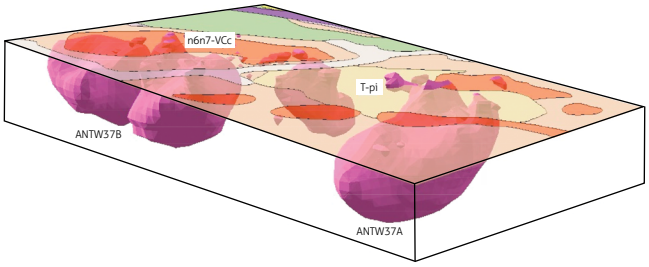

Figure 8. 3D susceptibility model for the magnetic source ANTW37B associated on the surface with the basalts of the Combia Formation (n6n7-VCc)

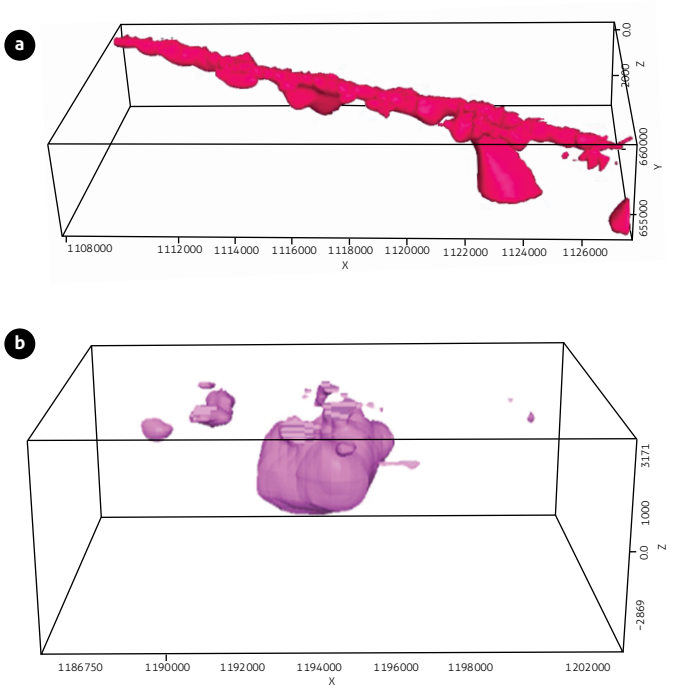

Figure 7. Example of possible geological sources (a) Dike, (b) Intrusive

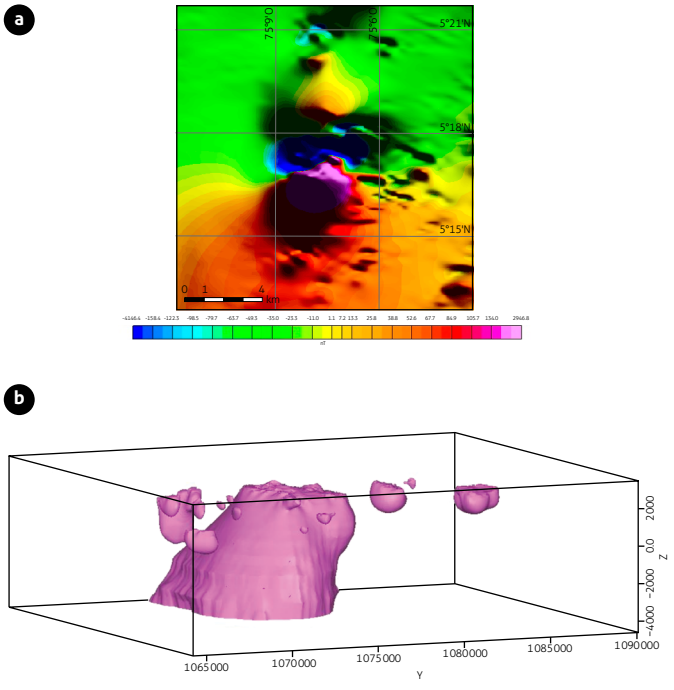

Figure 9. a) Plan view ACT map of the magnetic source ANDN011 b) 3D susceptibility model for the magnetic source ANDN011

Based on the integration of the geological and metallogenic contexts and the response or geophysical signature of each of the magnetic sources modeled**,** five possible geological sources are proposed for the MAGC 2020 (Moyano et al., 2020): dike (faults, veins and structural pattern), Intrusive, lithological, sedimentary and deposit model (DM). Thus, it is possible to advance the hypothesis that magnetic sources with geophysical characteristics and a similar geological-metallogenic context to those identified as DM may offer an exploratory potential similar to that already established based on the current geological knowledge of the existing deposits.

The differentiation of the possible exploration targets was based mainly on the identified deposit models (DM), and also taking into account parameters of the magnetic sources, such as magnetic susceptibility, depth and vertical extension, geometry and other geophysical attributes observed during the geophysical interpretation, together with the information from the MMC 2020 (Sepulveda et al., 2020) and the 2015 version of the Geological Map of Colombia (Gómez et al., 2015).

Seven possible exploratory targets were defined: intrusive, porphyry, mafic and ultramafic rocks (including laterites), carbonatites, kimberlites and placer deposits. Magnetic sources associated with a surface lithological response, and identified as such in the field as a possible geological source, were not considered.

4. Discussion

The maps were generated by processing the airborne geophysical magnetometry and gamma spectrometry data acquired in 17 blocks between 2018 and 2020. Magnetic anomalies were selected based on the TFMA map dipoles, and 3D inversion models of each were created. This process resulted in a distribution of magnetic susceptibilities related with magnetic bodies in deep and shallow zones with induced and remnant magnetization, defined as *magnetic sources*, while at the surface, the radioelement ternary gamma spectrometry data enhanced the lithological contrasts.

The maps obtained from the TFMA (Figure 2) of the different zones show the variation in the magnetic field due to the different geological structures. The magnetic anomalies of the Eastern zone are, for the most part, broader than the anomalies of the Andean and Caribbean zones. This finding indicates a clear differentiation of lithologies between the eastern region and the others.

Similarly, the AS shows the location of the bodies causing the magnetic anomalies (Figure 3), in addition to their plan shape. Therefore, the AS shows the extent of the rock formations and the limits of the heterogeneous geological formations and tectonic characteristics (faults). Thus, the AS of the Andean and Caribbean zones shows marked trends in the orientation of their magnetic structures, as is evident in the Urabá-Antioquia West and Bolívar and Cesar-Perijá blocks, in which tectonic activity is present. In addition, the analytic signal shows important geological structures, such as the Antioquia Batholith, which is located in the Antioquia west and East blocks, as in in Figure 10.

The AS of the eastern zone reveals a varied orientation and broad magnetic structures. The high AS values indicate a high gradient in three spatial components and strong contrasts in the magnetic susceptibility of the crystalline basement rocks. Magnetic structures such as extensive dikes are also observed, as shown in Figure 11.

These modeled sources have an estimated susceptibility ranging from 0.0001 to 0.09 SI and can estimate the shape of the source. According to the MVI models, the minimum magnetic susceptibility values were found mainly in the Amazonas S, Amazonas N, Vichada N and Buenaventura blocks (values lower than 0.0005 SI), while the highest susceptibility values were found in the GUAE, GUAINIA, ANTW and URABÁ blocks (values greater than 0.06 SI).

Let us note that the magnetic susceptibility model obtained by inversion represents only one of the several possible solutions that satisfy the predicted mathematical fit. Therefore, the susceptibility on which the geometric parameters of each magnetic source are estimated presents an uncertainty that can be progressively reduced, as long as there are control parameters over the area of interest, such as geological controls and magnetic susceptibility measurements of the rocks present in the area (petrophysics). With regards to the map of Colombian magnetic sources, the geophysical anomalies were interpreted during the early stages of evaluating the mineral resource potential, and as a guide to identifying those areas in which detailed field work may be carried out. Indeed, this type of control information is not always available, therefore the selected magnetic susceptibility has been estimated via parameters such as the anomaly geometry in layers, e.g., the analytic signal layer.

The possible geological source defined for each of the magnetic sources shows that most of them (82.3%) are of an intrusive type distributed throughout all zones, while 8.3% are

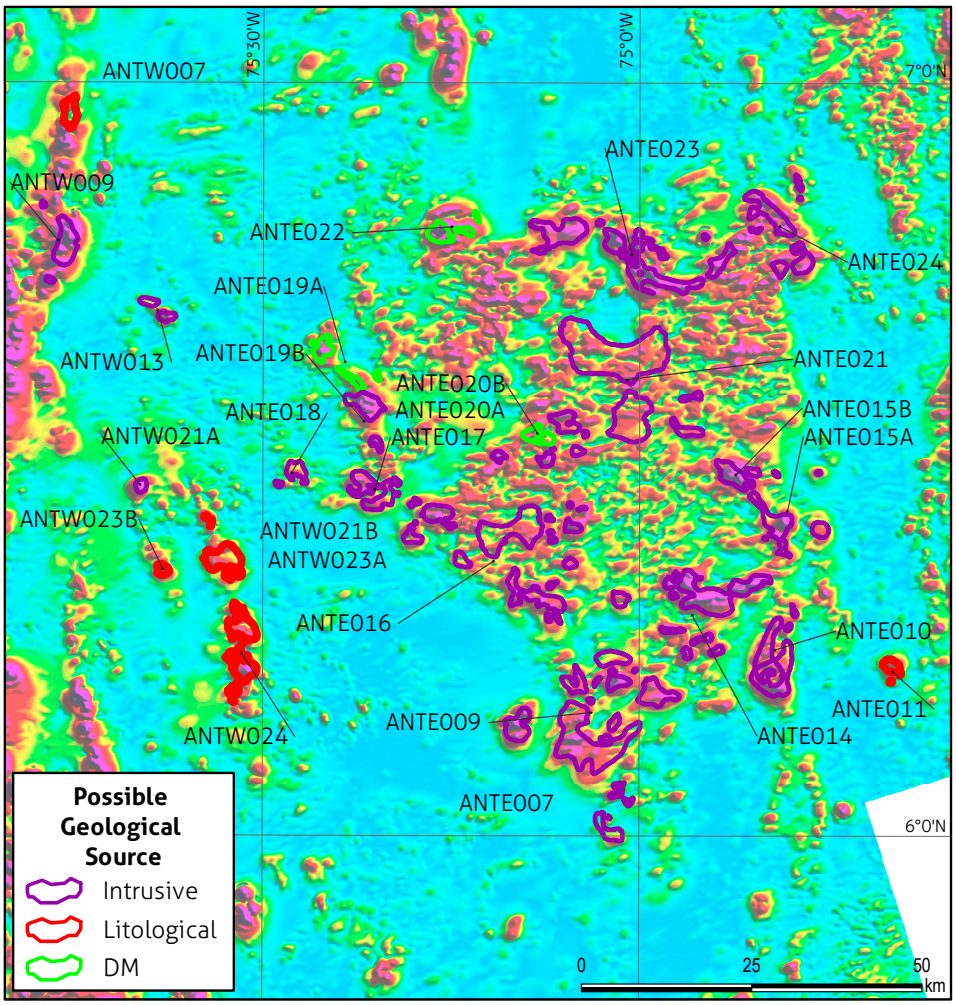

Figure 10. Possible geological sources in Antioquia Batholith
See general location in Figure 3.

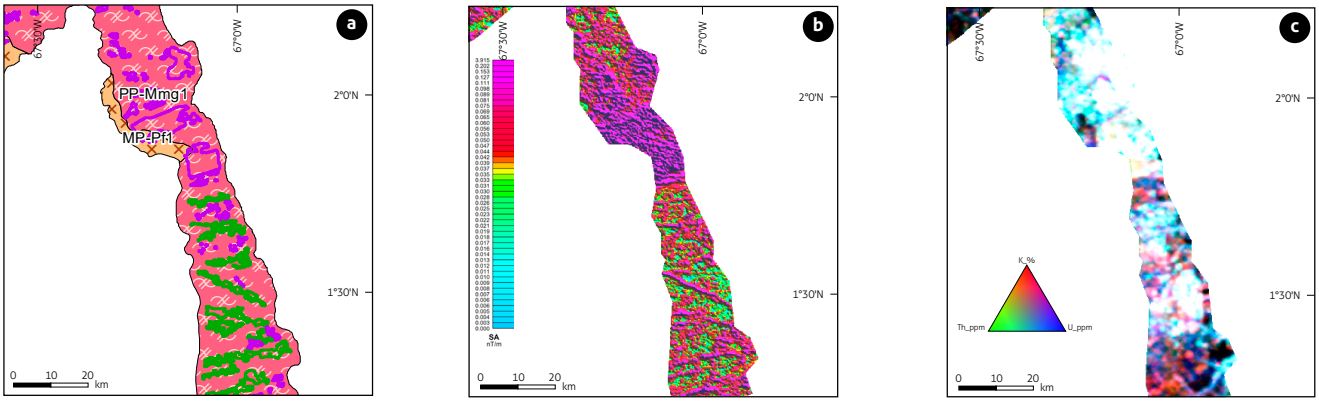

Figure 11. Left: Distribution of possible geological sources, intrusive (purple), and dike (green) of the eastern zone. Right: Analytic signal (AS) with magnetic sources of the eastern zone
a) Distribution of possible geological sources: Intrusive (purple), Dike (green), Chronostratigraphic units: PP-Mmg1: Complejo migmatítico de Mitú; MP-Pf1: Granito tipo Parguaza. b) Analytic signal map (AS) with distribution of possible geological sources: Intrusive (purple), Dike (green); c) Ternary map distribution of the potassium (K), thorium (Th) and uranium (U). See general location in Figure 1.

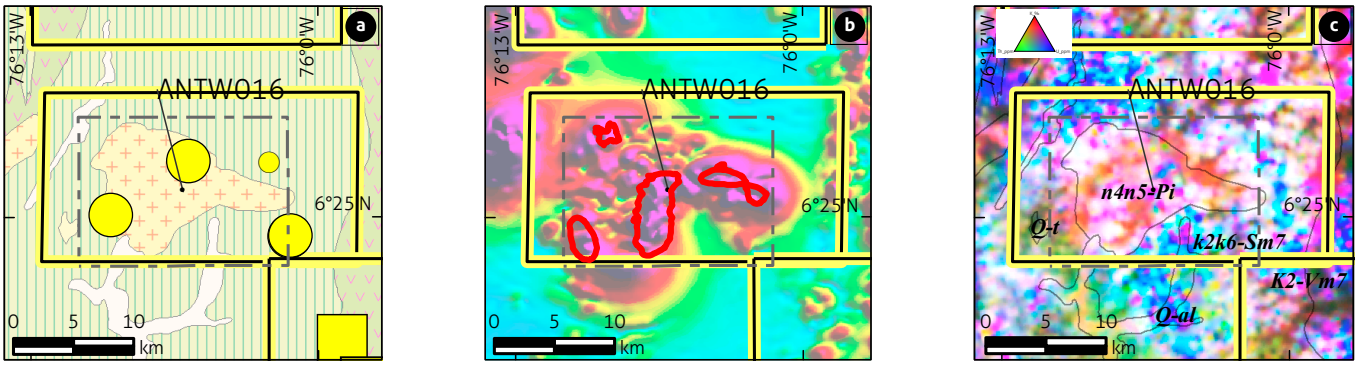

Figure 12. Magnetic source ANTW016 located in Antioquia W block, Páramo de Frontino area, identified as possible lithological geological source, and its distribution concentrations for radiometric elements of surface potassium (K), thorium (Th) and uranium (U)
a) Magnetic source: ANTW016 n4n5-Pi (La Horqueta Monzodiorite). Metallogenic District: Páramo de Frontino. Yellow circles: unclassified gold deposits; b) Analytical signal map (AS) with localization of magnetic source: ANTW016. Metallogenic District: Páramo de Frontino; c) Ternary map of the distribution potassium (K), thorium (Th) and uranium (U) n4n5-Pi La Horqueta Monzodiorite. Metallogenic District: Páramo de Frontino. See general location in Figure 5.

lithological and 1.7% are deposit models (DM). These magnetic sources are located mainly in the Andean and Caribbean zones. Finally, 7.6% are of the dike type and 0.1% of the sedimentary type, and are located mainly in the eastern zone.

Similarly, intrusive exploration targets constitute a higher proportion than other targets (54.6%). The porphyry type and mafic and ultramafic rocks comprise respectively 12% and 25.4% of the targets, and are associated with possible targets for kimberlites, carbonatites and veins, while the remaining 8% comprises the possible exploration targets of the placer, veins and lithologic types.

In addition, gamma spectrometry information shows different combinations of radiometric element concentrations for surface potassium (K), thorium (Th) and uranium (U). The gamma spectrometry RGB composite ternary map reflects the chemical composition of rocks and soil and may indicate lateral changes in said composition (Figure 5). These changes can be related to different lithologies (igneous, metamorphic and sedimentary), which reflect the regional tectonic processes and events that occurred in the area under consideration. Similarly, the ternary map may help to identify areas that have experienced alterations owing to the action of fluids during mineral accumulation processes. These alterations may be related to areas of high or low concentrations of radioelements, identified as light or dark areas in the ternary map, respectively. An example of the above is the magnetic source ANTW016 located in Antioquia W block, sector Páramo de Frontino shown in Figure 12. Additionally, areas enriched with potassium as a result of hydrothermal alteration are identified by red tones in this same map.

The gamma spectrometry data of the Eastern zone can be correlated with the lithological units already described and mapped, or with unidentified geological units. However, the limits between contrasts may not correspond to contacts between different lithostratigraphic units, but to variations or alterations within the same geological unit. It should be noted that gamma spectrometry data are sometimes of low resolution as a result of flight altitude issues owing to the steep topography of the Andean and Caribbean zones.

5. Conclusions

Magnetometry and gamma spectrometry data processing techniques were effective in producing geophysical coverage maps that can provide new geological information and detect the potential existence of mineral resources. These techniques are also a valuable tool for land-use planning related to the national territory.

The acquisition and processing of magnetometry data in 17 airborne geophysical blocks enabled the identification and modelling of 1297 magnetic sources associated with bodies with induced magnetization and magnetization perpendicular to the magnetic field. Based on the magnetic sources, potential mineral deposit sites were identified, either covered or outcropping, based on their distribution, depth, size, shape, and modeled magnetic susceptibility.

From the gamma spectrometry data, a ternary map showing the distribution of potassium (K), thorium (Th) and uranium was generated. This map can be used to identify new outcropping geological units according to the concentrations of these radioelements, and to generate and interpret new information, such as lithogeophysical maps. To do so, it is necessary to integrate this information with geological data to complement the geological mapping information of the country.

Acknowledgments

The authors thank the Servicio Geológico Colombiano for the managerial initiative and the financial, administrative and technical support in collecting the information, which will support Colombia's technical and scientific development. The anonymous reviewers are thanked for their contributions and suggestions which have helped to improve the article.

References

Baranov, V. (1957). A New Method for Interpretation of Aeromagnetic Maps: Pseudo-Gravimetric Anomalies. *Geophysics, 22*(2), 359-383. https://doi.org/10.1190/1.1438369

Briggs, I. C. (1974). Machine contouring using minimum curvature. *Geophysics*, *39*(1), 39-48. https://doi.org/10.1190/1.1440410

Ellis, R., Wet, B., & Macleod, I. (2012). Inversion of Magnetic Data from Remanent and Induced Sources. *ASEG Extended Abstracts, 2012*(1). https://doi.org/10.1071/ASEG2012ab117

Gómez, J., Montes, N. E., Nivia, A., & Diederix, H. (2015). *Mapa geológico de Colombia 2015, Escala 1:1 000 000*. Servicio Geológico Colombiano.

Gunn, P. J., & Almond, R. (1997). A method for calculating equivalent layers corresponding to large aeromagnetic and radiometric grids. *Exploration Geophysics, 28*(1-2), 72-79. https://doi.org/10.1071/EG997072

International Atomic Energy Agency. (2003). *Guidelines for radioelement mapping using gamma ray spectrometry data*.

Minty, B. R. S. (1991). Simple micro-levelling for aeromagnetic data. *Exploration Geophysics*, *22*(4), 591-592. https://doi.org/10.1071/EG991591

Moyano, I., Lara, N., Arias, H., Gómez, E., Ospina, D., Puentes, M., Robayo, A., Rojas, O., & Torrado, S. (2020). *Mapa de anomalías geofísicas de Colombia para recursos minerales. Escala 1:1 500 000*. Servicio Geológico Colombiano.

Moyano, I., Lara, N., Puentes, M., Rojas, O., & Cardenas, L. (2016). *Mapa de anomalías geofísicas de Colombia para Recursos Minerales, versión 2016. Escala 1:1 500 000.* Servicio Geológico Colombiano.

Moyano, I., Lara, N., Ospina, D., Salamanca, A., Arias, H., Gómez E., Puentes, M., & Rojas, O. (2018). *Mapa de anomalías Geofísicas de Colombia para Recursos Minerales, Versión 2018. Escala 1:1 500 000*. Servicio Geológico Colombiano.

Nabighian, M. N. (1972). The analytic signal of two-dimensional magnetic bodies with polygonal cross-sections: it´s properties and use for automated anomaly interpretation. *Geophysics*, *37*(3), 5074-517. https://doi.org/10.1190/1.1440276

Roest, W. R., Verhoef, J., & Pilkington, M. (1992). Magnetic interpretation using 3-D Analytic Signal. *Geophysics*, *57*(1), 116-125. https://doi.org/10.1190/1.1443174

Sepúlveda, J., Celada, C. M., Gómez, M., Prieto, D., Murillo, H., Rodríguez, A., Rache, A., Jiménez, C. A., Velásquez, L., Luengas, C., Torres, C., García, D., Prieto, G., Peña, L., Leal-Mejía, H., & Hart, C. (2018). *Mapa metalogénico de Colombia versión 2020. Escala 1:1 500 000*. Servicio Geológico Colombiano.

Thébault, E. et al. (2015). International Geomagnetic Reference Field: the 12th generation. *Earth, Planets and Space*, *67*, 79. https://doi.org/10.1186/s40623-015-0228-9

Watson, D., & Philip, G. M. (1985). A Refinement of Inverse Distance Weighted Interpolation. *Geoprocessing*, *2*(4), 315-327.